DANMARKS OG GRØNLANDS GEOLOGISKE UNDERSØGELSE RAPPORT 2019/22

CO_2 Neutral energy system utilising the subsurface

WP3 Evaluating chemical reactions upon seasonal heat storage in the hot deep Gassum Sandstone Formation, Aalborg, Denmark

Hanne Dahl Holmslykke, Rikke Weibel & Dan Olsen

GEOLOGICAL SURVEY OF DENMARK AND GREENLAND
DANISH MINISTRY OF CLIMATE, ENERGY AND UTILITIES

GEUS

DANMARKS OG GRØNLANDS GEOLOGISKE UNDERSØGELSE RAPPORT 2019/22

CO_2 Neutral energy system utilising the subsurface

WP3 Evaluating chemical reactions upon seasonal heat storage in the hot deep Gassum Sandstone Formation, Aalborg, Denmark

Hanne Dahl Holmslykke, Rikke Weibel & Dan Olsen

GEOLOGICAL SURVEY OF DENMARK AND GREENLAND
DANISH MINISTRY OF CLIMATE, ENERGY AND UTILITIES

GEUS

Executive summary

The possibility of storing heated formation water in deep hot aquifers is investigated with laboratory experiments. In particular, geochemical reactions expected to take place upon injection of the heated formation water is tested with focus on potential heat promoted dissolution and precipitation processes in the Upper Triassic – Lower Jurassic Gassum Formation in the Aalborg area. The Gassum Formation is a roughly 200 meter thick geological formation rich in sandstones and with very good reservoir (aquifer) properties. It occurs in approximately 1500 meters depth below the Aalborg area.

A core flooding experiment at *in situ* pressure and the temperatures 23°C, 60°C, 80°C, 100°C, and 120°C has been conducted to simulate the injection of heated formation water. To represent one of the most abundant Danish geothermal reservoirs, core material from the Upper Triassic – Lower Jurassic Gassum Formation in the Farsø-1 well is used for the laboratory experiments. A synthetic CO_2-bearing Farsø brine is used as the flooding fluid. Geochemical analysis of the effluent from the flooding experiment is combined with petrographic analysis of the sandstone before and after the experiment and provide input to a geochemical numerical model that constrain and support the interpretation of the results from the laboratory experiments.

The experimental data, petrographic analysis and geochemical modelling in this study indicate that reinjection of heated formation water into the Gassum formation in the Aalborg area may induce or enhance albitisation of microcline, dissolution of quartz, ankerite and barite and cause precipitation of calcite.

The main changes in the aqueous composition induced by heating of the brine are increased concentrations of silicium, iron and barium caused by the dissolution processes. Re-precipitation of silicium, barium and iron upon cooling of the brine is a potential risk and appropriate removal of these elements e.g. by filtration in the surface facility is essential to prevent clogging of the injection well to ensure a continuous heat production from the heat storage plant.

The concentration of aqueous silicium increases stepwise with increasing temperature from c. 1 mg/L at 60°C to c. 8 mg/L at 120°C. The silicium concentration at each temperature is controlled by a quasi-steady-state between kinetically controlled dissolution and/or precipitation of microcline, kaolinite and quartz combined with equilibrium with albite at temperatures ≥ 80°C. Both the conversion of microcline to albite and the dissolution of quartz increases with increasing temperature. However, only an insignificant fraction of the microcline and the quartz is expected to dissolve during a 6 month storage period at both 100°C and 120°C and therefore dissolution of microcline and quartz is not expected to deteriorate the reservoir properties. Similarly, the formation of albite is not expected to affect the reservoir properties, since the albite precipitates inside the feldspar or as overgrowths on the microcline and thus has little effect on the reservoir permeability. Dissolution of microcline may, however, lead to the formation of illite, especially at higher temperatures. Since illite is very fiberous, the formation of illite may have a damaging effect on the reservoir permeability. The geochemical model indicates that the effluent is supersaturated with respect to illite and thus that illite may potentially precipitate during the experiment, although not identified by the petrographical analysis.

The concentration of barium also increases stepwise with increasing temperature. Thus, the concentration of aqueous barium increases from c. 1 mg/L at 60°C to c. 20 mg/L at 120°C

and appears to be kinetically controlled by dissolution of barite. The concentration of aqueous iron increases from c. 10-15 mg/L at 60°C to c. 35 mg/L at 120°C and appears to be controlled by ankerite dissolution and calcite precipitation. Neither the dissolution of barite nor ankerite is expected to damage the formation, as these are present as cementing phases between framework grains in very small amounts in the reservoir.

In conclusion, the results of this study show that the dissolution/precipitation processes that may potentially be induced by storage of heated formation water with temperatures up to 120°C in the Gassum Formation in the Aalborg area are not likely to damage the reservoir and that heat storage in this reservoir may be possible provided operational precautions are taken.

Content

1 Introduction

This report summarises the results of the WP3 Reservoir characterisation and geo-model development in the project CO_2 neutral energy system utilising the subsurface (CONVert). This part of the project provides a detailed investigation of the possibility of storing heated formation water in deep hot aquifers with special focus on the chemical reactions expected to take place upon injection of the heated formation water. The project consists of the following three tasks:

- Laboratory tests of the geochemical reactions of hot water injection into sandstone
- Petrographical study of mineral reactions caused by hot water injection
- Geochemical modelling

The authors acknowledge the Danish energy technology development and demonstration research programme EUDP for funding "CO_2 Neutral Energy system utilising the Subsurface" (CONvert).

2 Background

Typically, a temporal incongruity exists between the supply and the demand for heat. Excess heat is for example produced from power generation during the summer, while the demand for energy peaks during the winter. This mismatch between the supply and the demand for heat may be managed by seasonal storage of the surplus heat in the subsurface. Thus, in seasonal heat storage formation water is extracted from the aquifer during the summer and heated using the available surplus energy prior to reinjection into the reservoir. In the winter, the heated formation water stored in the reservoir is extracted and used for e.g. district heating.

The idea of storing heat in the subsurface began in the 1960-ties and today aquifer thermal energy storage (ATES) is used in countries with suitable geological subsurface conditions e.g. the Netherlands. The ATES facilities operate in the depth of up to 500 meters. Due to a geothermal gradient of roughly 25-30°C/1000 meter in the Danish area the temperature will be maximum 25 degrees in Danish ATES facilities. To limit the thermal loss, the use of deep aquifers (>1000 meters) for storage of heated water is considered. It is the hypotheses that the energy loss will be minimised by injecting heated formation water into an aquifer that already contains formation water with a temperature between 35-50°C.

It is well known that temperature exerts an important control on mineral solubility as well as the extent and rate of chemical reactions between the reservoir minerals and the formation water. Generally, chemical reaction rates increase with increasing temperatures, whereas mineral solubility may either increase or decrease, depending on the thermodynamic properties of the mineral (Gruber et al., 2016; Appelo and Postma, 2005; Hoyer et al., 1994; Griffioen and Appelo, 1993; Brons et al., 1991; Dove and Crerar, 1990). For example, the solubility of silicates increases at elevated temperatures, while the solubility of carbonates decreases. The effects of the temperature becomes more pronounced at higher temperature differences due to the exponential dependence of reaction rates on temperature (Appelo and Postma, 2005; Palandri and Kharaka, 2004). A major concern regarding heat storage in the hot deep aquifers is that the heat may permanently damage the reservoir making extraction of further geothermal energy unfeasible. For example, dissolution of the cementing material in the sandstone may reduce the mechanical strength of the reservoir and the heat or the associated dissolution/precipitation processes in the sandstone may affect the permeability by changing the pore connectivity and the pore space geometry (Schembre and Kovscek, 2005; Tenthorey et al., 1998; Moore et al., 1983).

Laboratory (Holmslykke et al., 2017b; Schepers and Milsch, 2013; Gong et al., 2012; Fu et al., 2009; Schembre and Kovscek, 2005; Azaroual and Fouillac, 1997) and field (Hoyer et al., 1994; Perlinger et al., 1987) tests reveal that at elevated temperatures up to 150°C, the release of silicium increases sharply due to dissolution of quartz and feldspars, while precipitation of several secondary minerals, including kaolinite, boehmite, gibbsite, and montmorillonite also has been observed. Field tests of heat storage at temperatures up to 150°C in a confined shallow calcite containing sandstone reservoir reveals precipitation of calcium carbonate due to the increased temperature to be the most critical problem, and a reduction of the calcium concentration was necessary to prevent scaling in the heat exchanger and storage well (Hoyer et al., 1994; Perlinger et al., 1987). Recent studies show, however, that reducing the calcium concentration may lead to a dissolution of the cementing calcite, which may ultimately reduce the mechanical strength of the geological formation (Holmslykke et al., 2019b).

Several potential geochemical reactions may be anticipated when injecting heated formation water into the reservoir; hence, laboratory tests are crucial to determine the actual reactions likely to occur at each potential heat storage site. In addition, the rate, extent and coupling of these reactions may also be predicted from laboratory experiments.

3 Work-flow

In this study, a detailed investigation of the possibility of storing heated formation water in deep hot aquifers is made with special attention on the geochemical reactions likely to occur upon injection of the heated formation water. Focus is on heat promoted dissolution and precipitation processes in the Upper Triassic – Lower Jurassic Gassum Formation in the Aalborg area. A core flooding experiment at reservoir conditions and elevated temperatures has been conducted to simulate the injection of heated formation water. Geochemical analysis of the effluent of the flooding experiment is combined with petrographic analysis of the sandstone before and after the experiment and provide input to a geochemical numerical model that constrain and support the interpretation of the results from the laboratory experiments (Figure 3.1).

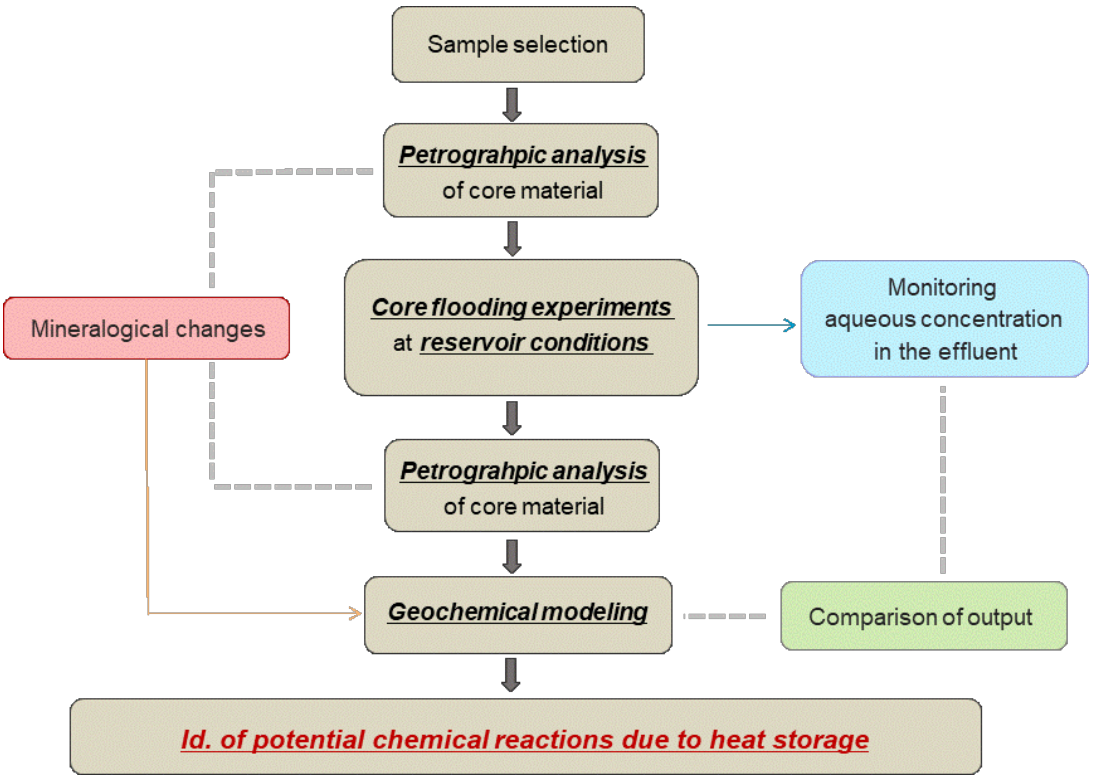

Figure 3.1 *Flow diagram of the tasks of the project.*

4 Materials and methods

4.1 Geological description

To represent one of the most abundant Danish geothermal reservoirs, core material from the Upper Triassic – Lower Jurassic Gassum Formation was selected for use for the laboratory experiments. The Late Triassic to Early Jurassic Gassum Formation was deposited in a shallow marine embayment under the influence of a number of relative sea-level fluctuations leading to deposition of shoreface sandstones and fluvial–estuarine sandstones interbedded in marine, lagoonal and lacustrine mudstones (Nielsen, 2003). The formation is widely distributed onshore Denmark (Fig. 4.1). Its thickness varies from 50–150 m in the central and distal areas of the Danish part of the basin, with thickening near salt-structures and major faults (up to 300 m in the Sorgenfrei–Tornquist Zone (Nielsen and Japsen, 1991). On the Skagerrak–Kattegat Platform the thickness decreases (10–80 m) and the formation is absent on most of the Ringkøbing–Fyn High due to later uplift and erosion (Nielsen, 2003). The Gassum Formation is characterized by a mature mineralogical composition with a dominance of quartz (Weibel et al., 2017a; Weibel et al., 2017b). The content of feldspar vary across the basin, being lowest in the eastern part. The Gassum Formation is represented in cores with present day burial depths from 800 – 6000 m (Weibel et al., 2017a) and up to 800 m deeper maximum burial depth (Japsen et al., 2007). The degree of cementation increases with burial depth and consolidated plugs can be retrieved from sandstones from deeper than 2000 m present day burial depth.

4.2 Sample material and fluid

Several deep wells penetrating the Gassum Formation exist in the Aalborg area. However, for most of the wells, collecting a representative sample suitable for laboratory experiments is not possible, as indicated in Table 4.1. Though the Gassum Formation in the Farsø-1 well has a deep burial depth, the mineralogy of the core material in the well is characteristic of the Gassum Formation in the Aalborg area. Therefore, a cylindrical specimen was prepared from a cored interval of the Upper Triassic – Lower Jurassic Gassum Formation in the Farsø-1 well (Figure 1) from a depth of 2874.2 m. The pre test parameters for the plug is shown in Table 4.2.

A syntethic Farsø brine is used as the flooding fluid for the laboratory experiment. The chemical composition of the synthetic Farsø brine is modified from Laier (2008) and is shown in Table 4.3. The silicium and aluminium concentrations were not measured by Laier (2008). A CO_2 gas content of 24% at 1 atm. was added to the synthetic brine corresponding to the expected CO_2 content of the brine *in situ* the reservoir (Laier, 1982). The salinity of the brine is 23.4% wgt %.

Table 4.1 Overview of deep wells in the Aalborg area

Well	Comments
Haldager-1	Core material from the Gassum Formation is unconsolidated and therefore not suitable for laboratory experiments.
Vedsted-1	Nearly all core material used in previous projects. A full size plug (7-7.5 cm long) could not be retrieved and the experimental plug would have had to be combined of several smaller plugs, which is not optimal for laboratory experiments.
Vendsyssel-1	No core in the Gassum Fm.
Flyvbjerg-1	Dominated by cementing siderite, which is not representative for Gassum Fm. in the Aalborg area.
Sæby-1	No core in the Gassum Fm.
Børglum-1	Core material from the Gassum Formation is unconsolidated and therefore not suitable for laboratory experiments.
Fjerritslev-2	A very short core in which the remaining part is mainly siderite-cemented. Application of such a sandstone would provide interesting though not representative results for the entire Gassum Formation.
Hyllebjerg-1	No core in the Gassum Fm.
Aars-1	Too deep burial depth and therefore too low permeability for the laboratory experiment.
Farsø-1	Deep burial depth (3000 m) but has a representative mineralogy and intervals with reasonably porosity and permeability.
Frederikshavn	Core material from the Gassum Formation is unconsolidated and therefore not suitable for laboratory experiments.

Table 4.2 Length, Diameter, Porosity and Gas permeability of the core specimen used for the laboratory experiment.

Well	Length mm	Diameter mm	Porosity %	Gas permeability mD
Farsø-1	56.6	24.85	15.7	86.2

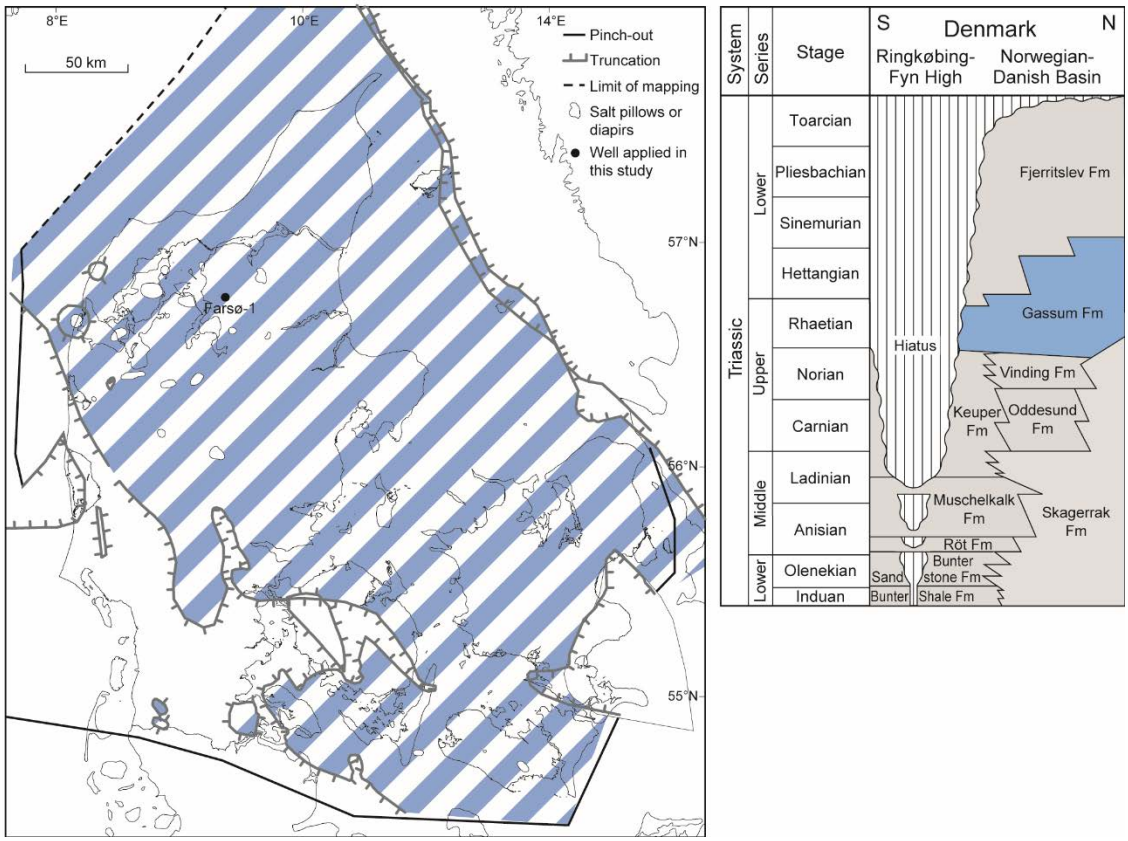

Figure 4.1 *Map of Denmark showing the extent of the Gassum Formation in blue colour (to the left) and the stratigraphic scheme (to the right). Modified from Weibel et al. (2017b).*

Table 4.3 Chemical composition of the synthetic Farsø brine used as the flooding fluid in the laboratory experiment. The chemical composition of the brine is modified from Laier (2008).

	Concentration (mg/L)
Na	73000
Ca	28000
Mg	2000
K	1600
Sr	920
Cl	169000
HCO_3^-	50
$SO4_2^-$	250

Figure 4.2 shows the pH of the synthetic Farsø brine containing CO_2 at temperatures up to 120°C. The pH is calculated with PHREEQC (Parkhurst and Appelo, 2013) using its Pitzer database and with the Thermoddem database (Blanc et al., 2007). The Thermoddem database is applied for the subsequent geochemical modelling of the experimental results as this database includes a large collection of relevant silica minerals and it is optimised to high temperatures. However, to calculate the activity coefficient of the ions in solution, the Thermoddem database uses the Debye-Hückel theory (Atkins and de Paula, 2002), which is only valid for

dilute solutions. Therefore, the pH is also calculated using the Pitzer database, since this database uses the Pitzer approach (Plummer et al., 1988; Pitzer, 1981) to calculate the ion activity which may be more appropriate in high salinity solution as the Farsø brine. However, the Pitzer database only includes an inadequate range of aqueous species and minerals, excluding many of the silica minerals relevant for this study.

The pH of the CO_2 containing Farsø brine is slightly acidic with a pH of about 5-6. The pH is 0.35 – 0.45 pH units lower depending on the temperature when calculated using the Thermoddem database as compared to the Pitzer database, which is attributed to the different methods to calculate the activity coefficients of the ions in solution. For both databases a slight increase in the pH is observed with increasing temperature due to the temperature dependency of the equilibrium constants of the aqueous species in solution.

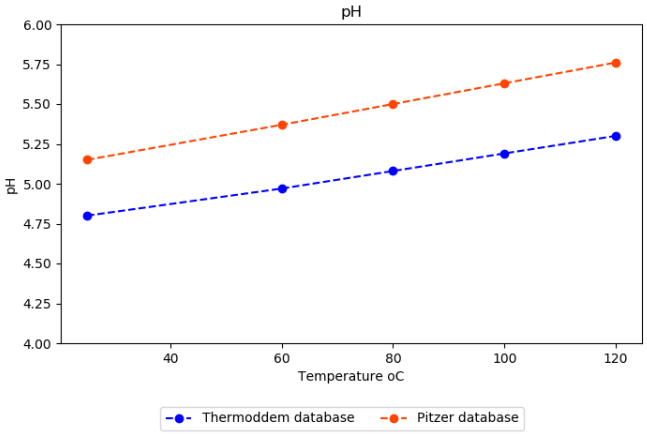

Figure 4.2 *Calculated pH of the synthetic Farsø brine (Table 4.3) containing 24% CO_2 at 1 atm. The pH is calculated with PHREEQC using its Pitzer database and the Thermoddem database.*

The saturation state of the synthetic CO_2 bearing brine at temperatures up to 120°C was tested by equilibrium calculations with PHREEQC (Parkhurst and Appelo, 2013) to test if any minerals were likely to precipitate prior to injection into the core sample during the core flooding experiment. The saturation state of the brine with respect to selected minerals is indicated by the Saturation Index (SI) in Figure 4.3 whereby positive and negative values indicate super-saturation and sub-saturation, respectively. From Figure 4.3 it is clear that the synthetic Farsø brine is sub-saturated with respect to celestite ($SrSO_4$) and anhydrite ($CaSO_4$) at all tested temperatures and therefore precipitation of these minerals are not expected. For calcite and dolomite the saturation indices increase with increasing temperature and when using the Pitzer database the saturation index for both carbonates indicates a potential risk of precipitation of the carbonate at elevated temperatures. However, when using the Thermoddem database the saturation index remains negative and does not indicate potential precipitation of either of the carbonates. Precipitates were not visually observed in the brine at room conditions.

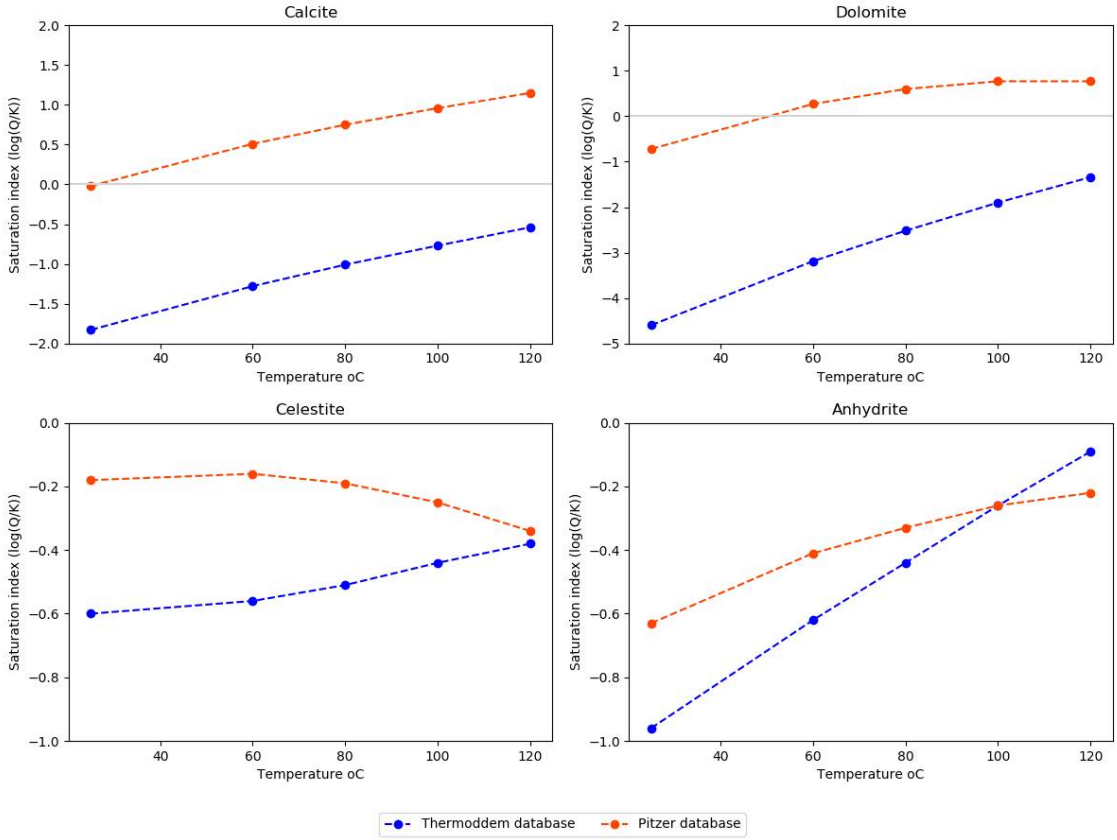

Figure 4.3 *Saturation indices (log(Q/K)) at temperatures up to 120°C for calcite ($CaCO_3$), dolomite ($CaMg(CO_3)_2$, celestite ($SrSO_4$) and anhydrite ($CaSO_4$) for the synthetic Farsø brine (Table 4.3) containing 24% CO_2 at 1 atm. The saturation indices are calculated with PHREEQC using its Pitzer database and the Thermoddem database. Positive and negative values indicate super-saturation and subsaturation, respectively.*

4.3 Experimental procedure

To simulate the injection of heated formation water into the reservoir, a core flooding experiment was performed, flushing a cored specimen from the Gassum Sandstone Formation in the Farsø 1 well with heated synthetic formation water at reservoir conditions and temperatures up to 120°C. Prior to testing, the specimen was cleaned in methanol to remove any salt precipitation. He-porosity, N_2-gas permeability and Klinkenberg permeability were measured (API, 1998) before and after the tests. Prior to testing, the specimen was vacuum (at -1 mbar) and pressure (at 110 bar for three days) saturated in degassed formation water without CO_2 and the saturation state of the specimen was verified using the Archimedes test. Upon testing, the brine saturated specimen was placed in a Viton sleeve in a hydrostatic core holder and connected to a high precision Quizix® pump assuring a constant flow with synthetic CO_2 bearing formation water (Table 4.3) at a rate of 0.25 PV/h (0.039 cm/h) through the specimen during the test (Figure 4.4). A confining pressure of 300 bar and a pore pressure of 145 bar were applied corresponding to the in situ lithostatic and hydrostatic pressure, respectively at a depth of 1400m. Tests were performed at room temperature, 60°C, 80°C, 100°C and 120°C.

Effluent brine for chemical analysis was collected from the sample collection loop placed downstream the core holder. During the experiment, flow was allowed to pass through the sample collection loop. At the time of sampling, the flow was shifted to bypass the sample collection loop, while maintaining the flow unchanged. In order to withdraw the sample, a secondary sampling loop was mounted outside the oven and pressurized to 145 bar by a N_2 gas ballast. The effluent brine in the sample collection loop was subsequently transferred to the sampling loop by injection of distilled water at 145 bar. The first few ml, being water from the downstream manifold of the sample collection loop to the valve connecting to the secondary sampling loop, was disregarded, as this does not represent effluent brine. After the transferral of the effluent brine, the sample collection loop was repressurised to 145 bar by injection of distilled water. The secondary sampling loop was allowed to cool to ambient temperature (23±1°C) if necessary, dismantled from the set up and the content of the loop transferred to a syringe.

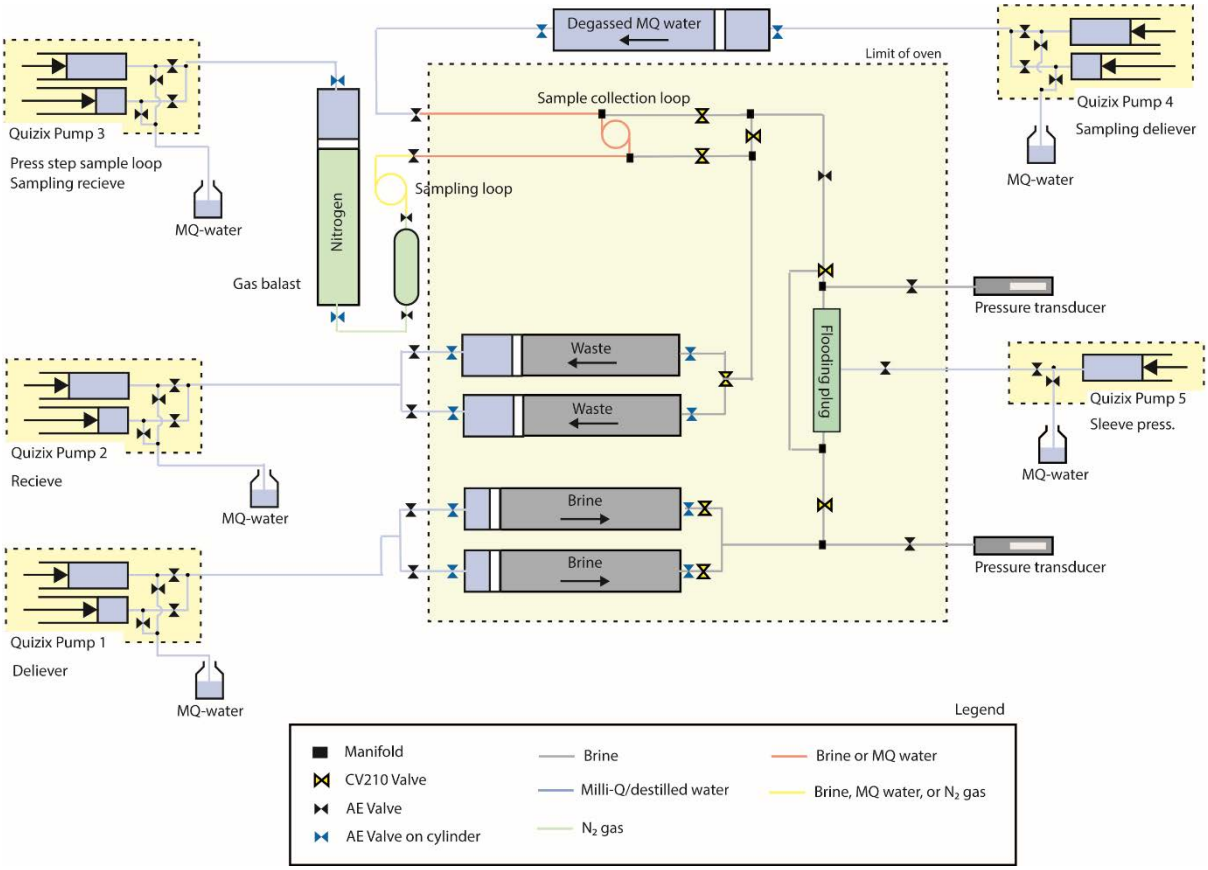

Figure 4.4 *Experimental set up*

The pH was determined immediately after extracting the effluent from the secondary sampling loop using a Mettler-Toledo InLab® Micro pro pH electrode, freshly calibrated against dilute standard pH buffers (pH 4-10, Merck). Samples for analysis of the content of aqueous species were passed through 0.22 µm cellulose-acetate syringe filter into two separate polyethylene vials. Samples for analysis for cations received 0.4 vol% of 7M HNO_3, and were kept refrigerated until analysis. Major cations (Na, K, Ca and Mg) were measured by ICP-MS (PerkinElmer Elan6100DRC Quadrupol) with a standard deviation of 3-15% depending on the element measured, Fe was measured by AAS (Perkin Elmer, AAnalyst 400- Atomic Absorption Spectrometer) with a detection limit of 0.016 mg/L, Al, Ba and other trace elements were measured by ICP-MS (PerkinElmer Elan 6100DRC, Elan software version 3.3) with a detection limit of 0.001-5 mg/L depending on the element. Samples for anion analysis (chloride

and sulphate) were kept refrigerated and analysed within 14 days by ion-chromatography (Metrohm IC, 819 detector, column Metrosep A sup. 5 – 150/4.0)) with a quantification limit of 0.05 mg/L. Samples for silicium analysis were also kept refrigerated until spectrophotometric analysis with a detection limit of 0.1 mg/L (Shimadzu 1800 spectrophotometer) according to the method in Public Health Association (1975).

Due to the high salinity of the Farsø brine, the measured pH value differs from the actual pH value of the sample as a result of changes in the activity coefficient caused by the high ionic strength and in the diffusion potential between the sample solution and the electrolyte solution (Fanghänel et al., 1996). Thus, when measuring the pH, only an experimental pH is found:

$$-\log[H+] = pH_{exp} + A \quad (1)$$

The parameter A includes the individual activity coefficient γ_{H+} and contribution from the variation of the liquid junction potential when measuring dilute pH buffer solutions for calibration and saline test solutions. For a given pH electrode system, junction electrolyte and temperature, A depends only on the composition and concentration of the test solution (Altmaier et al., 2003). The parameter A was determined by measuring pH_{exp} in 4.5 M salt solutions containing known concentrations of HCl (0.0 – 0.1M), and NaCl. The measured pH_{exp} was tested against the pH of the solutions calculated by PHREEQC version 3.0 (Parkhurst and Appelo, 2013) and its Pitzer database (Table 4.4) and the pH of the solution is this calculated as:

$$pH = pH_{exp} + 0.45 \quad (2)$$

Table 4.4 Determination of the parameter 'A' based on measured (pH_{exp}) and calculated (pH_{calc}) pH values using PHREEQC and its Pitzer database.

	pH_{exp}	pH_{calc}	A
0.1 M HCl/4.4 M NaCl	0.01	0.42	0.41
0.05 M HCl/4.45 M NaCl	0.25	0.73	0.48
0.02 M HCl/4.48 M NaCl	0.66	1.13	0.47
0.01 M HCl/4.49 M NaCl	0.97	1.43	0.46
0.005 M HCl/4.495 M NaCl	1.28	1.73	0.45
4.5M NaCl	6.07	6.54	0.47
Average			0.45

4.4 Mineralogical changes

Three plug samples were investigated in order to cover possible changes in the plug during the experiment; 1) prior to experiment, 2) after the experiment, close to inlet and 3) after the experiment, from the outlet. The sandstones were impregnated with blue epoxy, for easy identification of porosity, and prepared as polished thin sections prior to analyses in transmitted and reflected light microscope. Supplementary studies of dissolution features and paragenetic relationships were performed on platinum-coated rock chips mounted on stubs and on carbon-coated thin sections using a Zeiss Sigma 300 VP operating at 10–15 kV equipped with double Bruker energy dispersive X-ray spectrometers (EDS) with 30 mm^2 active areas. Modal composition of the sandstone was obtained by point counting 500 points, in addition to the porosity.

4.5 Geochemical modelling

To help identify which minerals may possibly dissolve and/or precipitate during the experiment the injection of heated formation water into the Gassum Formation was modelled using the 1D reactive transport code PHREEQC version 3.0 (Parkhurst and Appelo, 2013). The thermodynamic data from the Thermoddem database were used since this database is optimised to high temperatures and includes a large range of silica minerals. The Thermoddem database uses the Debye-Hückel theory (Atkins and de Paula, 2002) to calculate the activity coefficients of the ions in solution; an approach that is only valid for dilute solutions. For solutions of higher salinity, such as the Farsø brine, the Pitzer approach (Plummer et al., 1988; Pitzer, 1981) may sometimes be more appropriate to define activities based on specific ion interactions. However, the Pitzer database only includes an inadequate range of aqueous species and minerals, excluding many of the silica minerals relevant for this study. The Thermoddem database has previously been successfully applied in similar studies (Holmslykke et al., 2019b; Holmslykke et al., 2017b).

A 1D transport model column, comprising 8 cells with a length of 0.00706 m each, was constructed and flushed with synthetic CO_2 bearing Farsø brine (Table 4.3) at 23°C, 60°C, 80°C, 100°C and 120°C and at 145 bar pressure. Dispersion was not taken into account in the model. The mineralogical input to the model was defined by the mineralogical changes during the experiment observed by the petrographic analysis. The model included the thermokinetic processes of mineral dissolution/precipitation reaction using the kinetic rate law given by (Appelo and Postma, 2005; Palandri and Kharaha, 2004):

$$R = k \cdot \frac{A_0}{V} \cdot \left(\frac{m}{m_0}\right)^{0.67} \cdot (1 - \Theta) \quad (1)$$

where R is the dissolution/precipitation rate (mol/L/sec), k the overall rate constant (mol/m^2/sec), A_0 the initial surface area (m^2), V the liquid volume (L), m the remaining mass of mineral, m_o the initial mass and θ the mineral saturation ratio given by θ = IAP/K, where IAP is the ionic activity product and K the equilibrium constant. The term $(m/m_0)^{0.67}$ corrects for changes in reactive surface sites during the dissolution/precipitation process (Appelo and Postma, 2005).

The dependency of the rate constant k with temperature is calculated by the Arrhenius equation:

$$k = k_{25} exp\left[\frac{-E_a}{R}\left(\frac{1}{T} - \frac{1}{298.15}\right)\right] \quad (2)$$

where E_a is the activation energy (J/mol), k_{25} the rate constant at 25°C, R the gas constant (J/mol/K) and T the temperature (K).

The overall rate equation is a sum of multiple mechanisms of which those in pure water (neutral), and those catalysed by H^+ (acid) and OH^- (base) are included in the rate expression for the silicates (Palandri and Kharaha, 2004):

$$k = k_{25}^N exp\left[\frac{-Ea^N}{R}\left(\frac{1}{T} - \frac{1}{298.15}\right)\right] + k_{25}^A exp\left[\frac{-Ea^A}{R}\left(\frac{1}{T} - \frac{1}{298.15}\right)\right] a_H^{n_A} + k_{25}^B exp\left[\frac{-Ea^B}{R}\left(\frac{1}{T} - \frac{1}{298.15}\right)\right] a_H^{n_B} \quad (3)$$

where a_H the activity of H^+ and the indices N, A and B refer to neutral, acid and base mechanisms, respectively.

For carbonates the dissolution/precipitation mechanisms are catalysed by HCO_3^- and reaction rates depend on the CO_2 pressure (P_{CO2}) (Carbonate mechanism). The overall rate expression for carbonates is therefore:

$$k = k_{25}^{N} exp\left[\frac{-Ea^{N}}{R}\left(\frac{1}{T} - \frac{1}{298.15}\right)\right] + k_{25}^{A} exp\left[\frac{-Ea^{A}}{R}\left(\frac{1}{T} - \frac{1}{298.15}\right)\right] a_H^{n_A} + k_{25}^{C} exp\left[\frac{-Ea^{C}}{R}\left(\frac{1}{T} - \frac{1}{298.15}\right)\right] P_{CO2}^{n_B} \quad (4)$$

where the indices C refer to the carbonate mechanism.

For barite, the rate expression found in (Zhen-Wu et al., 2016) is applied to account for the effect of the ionic strength of the flushing brine:

$$R = A_0 \cdot A \cdot exp\left(\frac{-E_a}{RT}\right) \cdot \gamma_{H+} \cdot 10^{n_I\sqrt{I}} \cdot (1 - \Theta^n) \quad (5)$$

where R is the dissolution/precipitation rate (mol/L/sec), A_0 the initial surface area (m^2), A the Arrhenius pre-exponential factor (mol/m^2/s), E_a the activation energy (J/mol), R the gas constant (J/mol/K), T the temperature (K), γ_H the activity of H^+, I the ionic strength of the fluid, θ the mineral saturation ratio, and n an exponential factor equal to 0.2 for dissolution and 1 for growth.

For most minerals precipitation rate data are not available and therefore the same kinetic expression is assumed for both dissolution and precipitation processes (Cantucci et al., 2009). The initial amount of the minerals was calculated from the mineral content found by point counting and rate constants and the initial specific surface area of the minerals were found in the literature (Cantucci et al., 2009; André et al., 2007). The specific surface area was used to fit the model to the observed data.

5 Results and discussion

5.1 Water chemistry

Chemical analysis of the effluent from the core flooding experiment primarily show changes in the aqueous concentration of silicium, barium, and iron (Figure 5.1). The concentration of aqueous silicium increases immediately upon changes in the temperature after which a constant level is reached. Thus, upon heating the silicium concentration increases stepwise from c. 1 mg/L at 60°C to c. 8 mg/L at 120°C. The same levels in the concentration of aqueous silicium upon temperature increases is previous observed in laboratory core flooding experiments with temperatures up to 150°C (Holmslykke et al., 2019b; Holmslykke et al., 2017a). The concentration of aqueous barium show the same pattern as for silicium, however a higher level is reached for the barium concentration. Hence, the concentration of aqueous barium increases stepwise from c. 1 mg/L at 60°C to c. 20 mg/L at 120°C (Figure 5.1). The stepwise increase in the barium concentration with temperature is previous observed (Holmslykke et al., 2019b), though significant higher levels of silicium is observed in this study.

The concentration of aqueous iron demonstrates a completely different pattern compared to silicium and barium. After an initial peak in the concentration of aqueous iron at room temperature with a concentration up to c. 35 mg/L, the iron content appears to continuously increase from c. 10-15 mg/L at 60°C to c. 35 mg/L at 120°C with no obvious correlation with temperature increases (Figure 5.1). The concentration of manganese remains generally low and below 1 mg/L, except immediately after increasing the temperature to 60°C and 80°C, where the concentration of manganese peaks at a level of c. 1.7 mg/L and 3 mg/L. respectively (Figure 5.1).

Although the measured pH appears to increase slightly from c. 6 to c. 6.3 during the experiment, no apparent correlation is observed between the temperature and pH (Figure 5.1). Changes in the aqueous concentration of calcium, magnesium, potassium, sulphate, sodium and chloride was not observed probably due to the very high content of these elements in the synthetic brine and the relative small changes that any reaction would cause. The concentration of aqueous aluminium remains below the detection limit, which due to high dilution requirements is 5 mg/L.

5.2 Mineralogical changes

The sandstone is quartz-dominated with common K-feldspar and albite (Table 5.1). K-feldspar shows common dissolution features and albitization. Rock fragments are generally rare. Metamorphic rock fragments (1.25 vol% of the sandstone) are micaceous or with chlorite intergrown with quartz. The latter commonly show dissolution features of chlorite thereby liberating some of the quartz crystals. (Chlorite may comprise up to 5 vol% of the metamorphic rock fragments). Graphic granite and siltstones are rare. Heavy minerals, such as tourmaline, zircon and leucoxene-replaced Fe-Ti oxides, are rare.

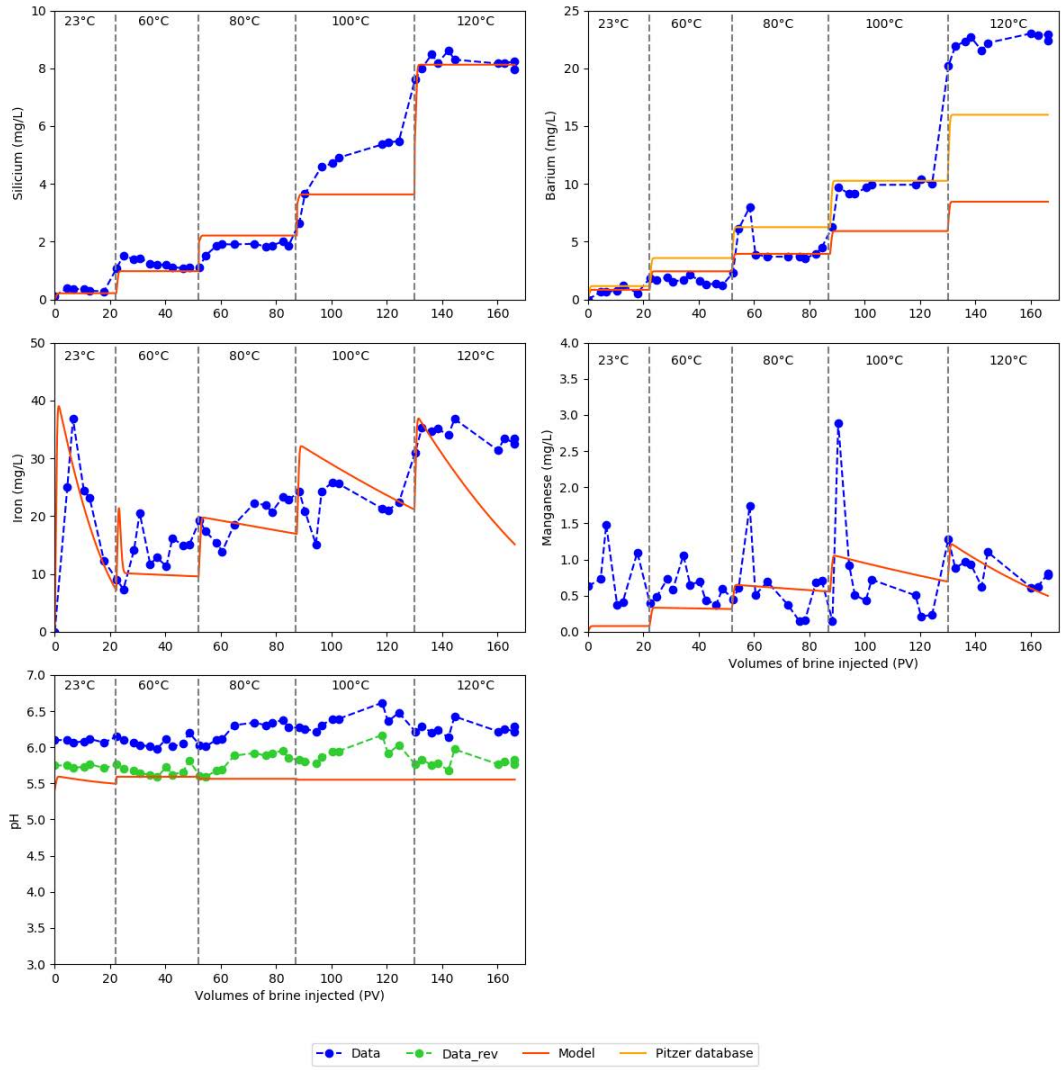

Figure 5.1 *Measured and modelled concentration of aqueous silicium, barium, iron, manganese and pH in the effluent of a core sample from the Gassum Formation in the Farsø-1 well flushed with synthetic CO_2-containing Farsø brine at temperatures 25°C, 60°C, 80°C, 100°C and 120°C and 145 bar and with a flow rate of 0.25 PV/h. The model includes kinetically controlled dissolution/precipitation of microcline, quartz, kaolinite, barite and ankerite together with equilibrium albite at temperatures ≥80°C and with calcite at all temperatures.*

Table 5.1: Mineral content in the tested plug determined by point counting 500 points.

Mineral	vol%
Quartz	69.5
K-feldspar	7.7
Albite	4.1
Muscovite	0.2
Rock fragments	2.3
Clay clasts	0.2
Heavy minerals	0.2
Kaolinite	1.8
Red coatings (goethite?)	0.2
Anatase	0.2
Ankerite	0.2
Porosity	13.5
TOTAL	100.0

Cementing phases are mainly quartz overgrowths, feldspar overgrowths, kaolinite, illite, ankerite and pyrite. Quartz overgrowths cover most detrital quartz grains (Figure 5.2). Albite occurs as overgrowths and replacement of K-feldspar. Kaolinite has typically formed close to altered feldspar grains (Figure 5.3). Illite occurs as a rare coating on detrital grains (Figure 5.4). Framboids of pyrite and tiny chalcopyrite crystals are rare. The experimental plug show possible copper-oxide alteration rim around chalcopyrite close to inlet. Anatase occurs as discrete crystals close to altered Fe-Ti oxides or enclosed in ankerite cement. Barite occurs as a rare cement occasionally with fractures (Figure 5.4) and is common as tiny crystals in drilling mud. Ankerite cement show more intense oxidation features at outer rim and along cleavage planes in the after-experiment samples (Figure 5.6). Occasionally, reddish outgrowths initiate at the rim of oxidised ankerite and continues into the open pores.

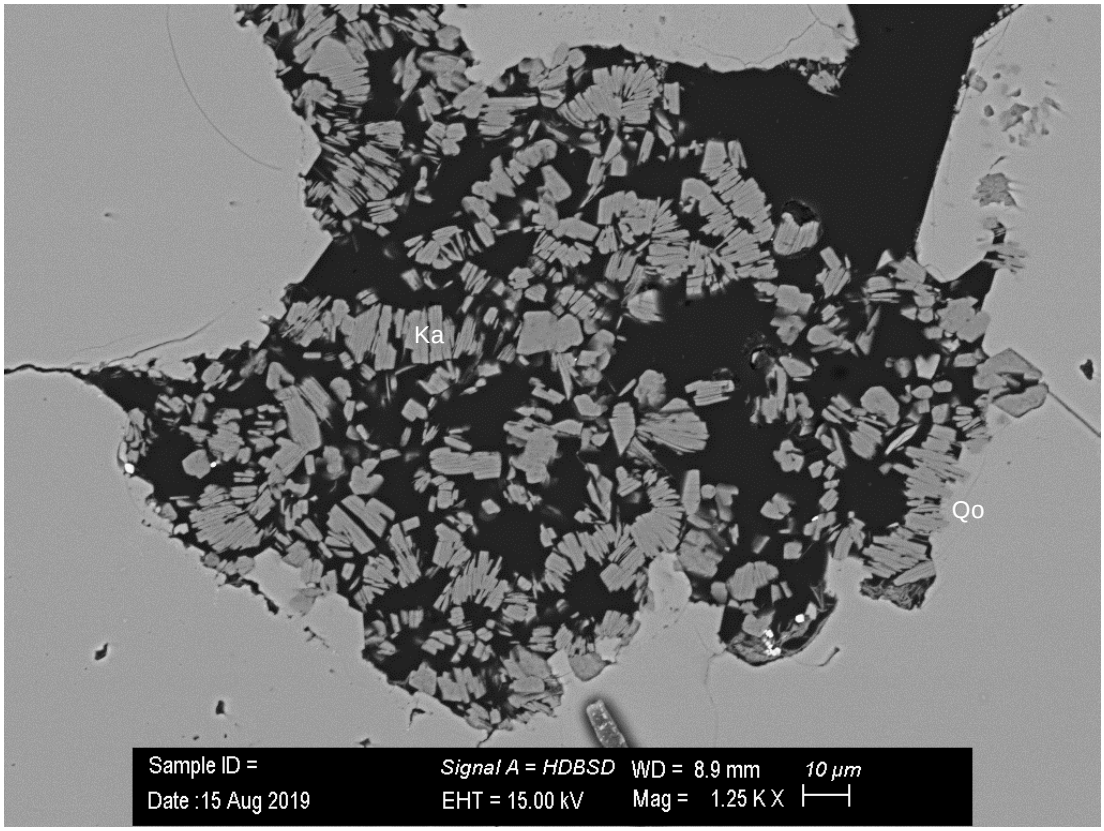

Figure 5.2 *Kaolinite (Ka) booklets occurring in large pore is locally enclosed in quartz overgrowths (Qo). Backscatter electron micrograph.*

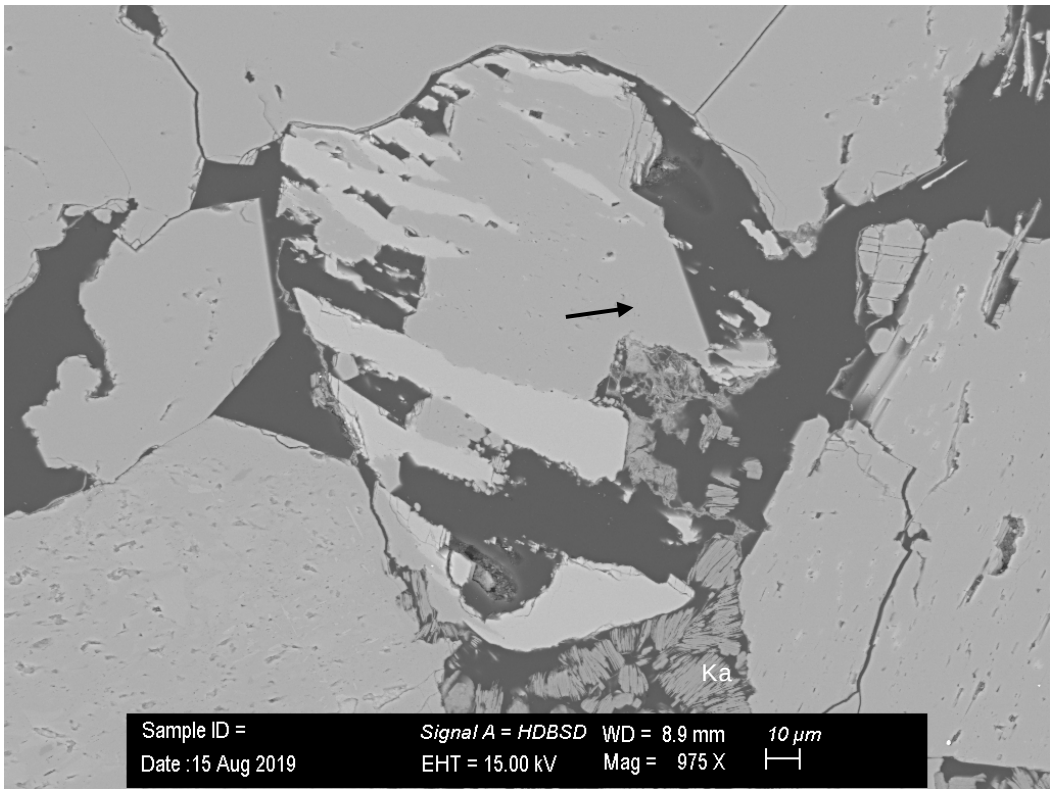

Figure 5.3 *Albite overgrowth (arrow) on partly dissolved intergrown K-feldspar-albite grain. Kaolinite (Ka) is forming in the pores next to the altered feldspar grain. Backscatter electron micrograph.*

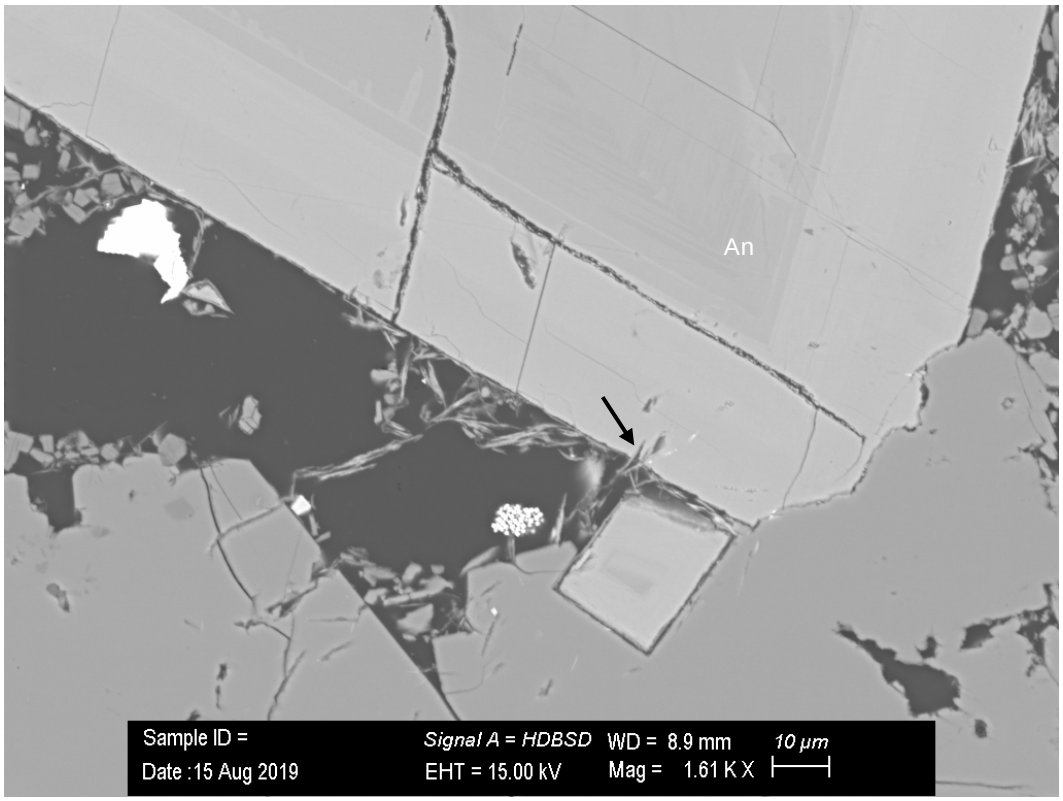

Figure 5.4 *Illite is partly enclosed (arrow) in the ankerite cement, which show clear zonation. It cannot be confirmed if illite also precipitated during the experiment. Backscatter electron micrograph.*

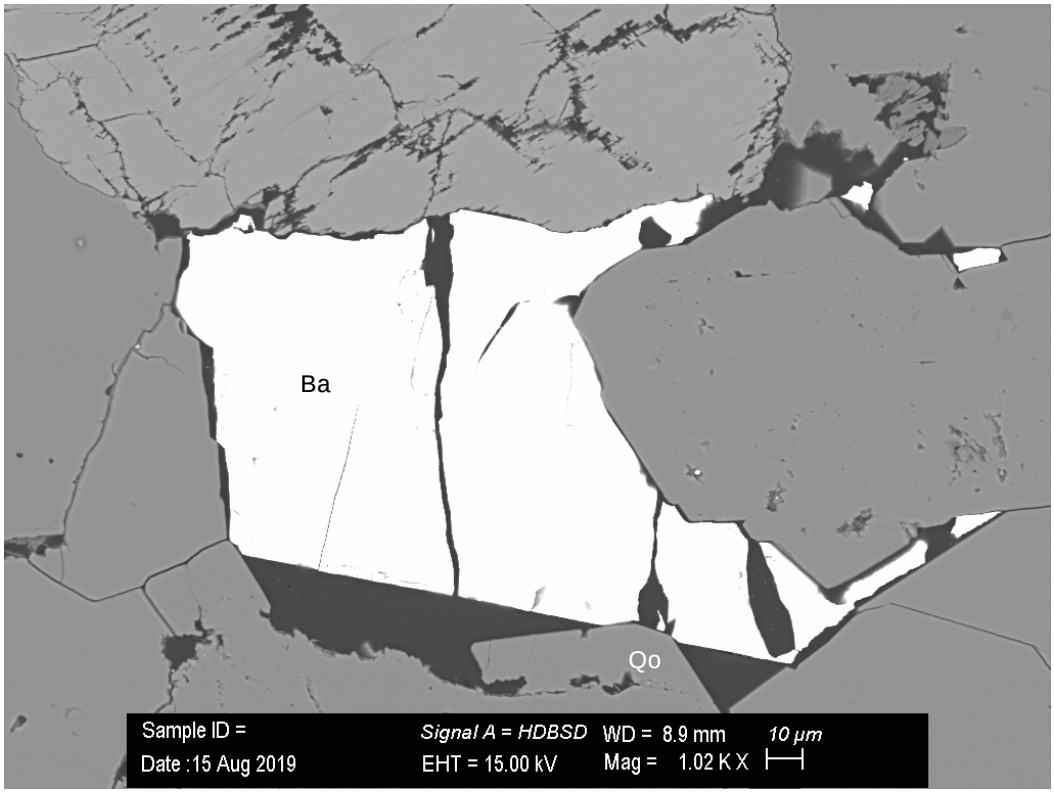

Figure 5.5 *Barite cement (Ba) with fractures and partly enclosing quartz overgrowth (Qo). Backscatter electron micrograph.*

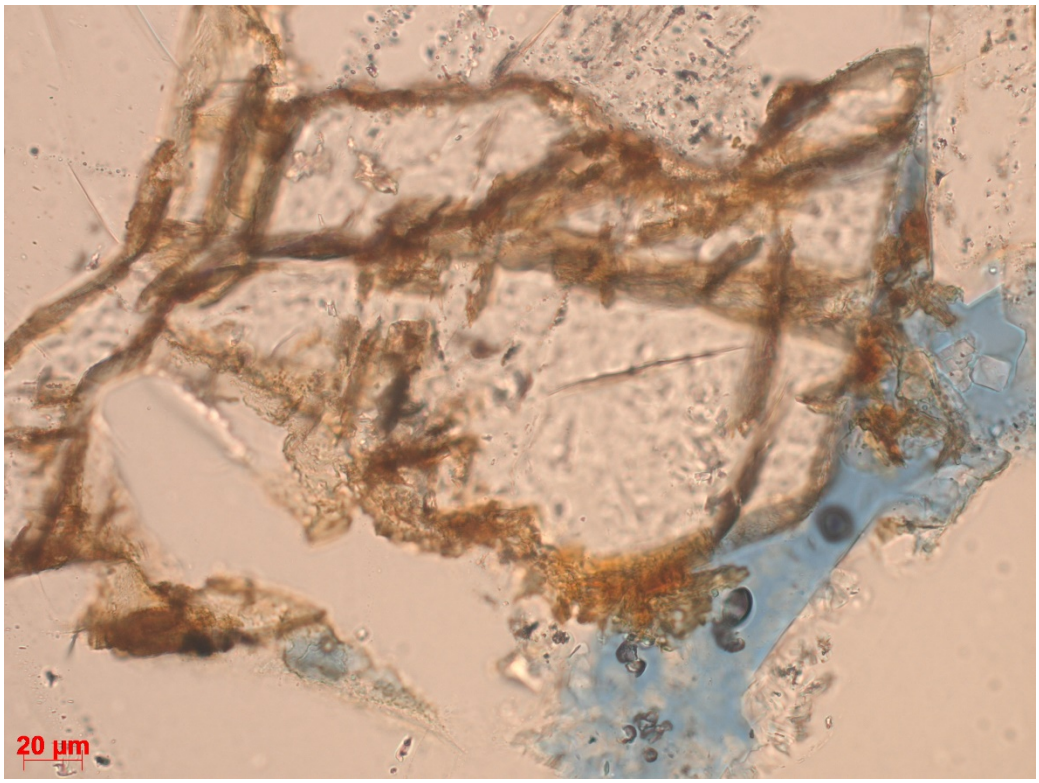

Figure 5.6 *Ankerite cement show oxidation along the outer rim and internal fractures.*

5.3 Geochemical modelling

Based on the petrographic analysis and the observed changes in the aqueous concentrations during the experiment, the geochemical model was fitted to the experimental data to help identify potential geochemical reactions upon injection of heated Farsø brine into the Gassum formation in the Aalborg area. The final model includes kinetically controlled dissolution/precipitation of microcline, quartz, kaolinite, barite and ankerite together with equilibrium with albite at temperatures ≥80°C and with calcite at all temperatures. The kinetic parameters are listed in Table 5.2. The initial amount of calcite was equal to 0 moles in accordance with the petrographic analyses.

The model was fitted to the experimental data by adjusting the specific surface area found in the literature (Cantucci et al., 2009). Generally, the specific surface area applied in the model is in accordance with the data found in the literature. Although the specific surface area for microcline obtained in this study is higher than reported in Cantucci et al. (2009), the value is still within the range found elsewhere in the literature (Holdren and Speyer, 1987). The specific surface area for kaolinite is, however, significant lower than reported in the literature, indicating a very low precipitation rate for kaolinite in this study. Kaolinite precipitates during the early diagenesis due to flushing of meteoric water (Weibel et al., 2017b). The high concentration of calcium, sodium and magnesium in this study may have a reducing effect on the precipitation rate of kaolinite (Peng and Di, 1994).

For barite the best fit of the model to the experimental data was obtained by applying the Arrhenius pre-exponential factor A = 1.6e-3 mol/m^2/s and the specific surface area A_0 = 0.002 m^2 in equation (5).

The results of the geochemical transport model fit reasonably well with the observed data (Figure 5.1). Additionally, in accordance with the measured aluminium concentration, the model predicts the concentration of aqueous aluminium to be significantly below the detection limit of 5 mg/L (due to high dilution requirements due to the high salinity of the brine). The model predicts the pH to be approximately 0.5 lower than the pH determined by equation 2 in which the Pitzer database was applied to determine the correction factor A. Calculating the pH in 4.5 M salt solutions containing known concentrations of HCl using both the Pitzer and the Thermoddem databases reveals, however, that at pH around 6, the Thermoddem database predicts the pH to be c. 0.45 lower than does the Pitzer database. Taken this difference into account the measured and the modelled pH fits reasonable well (the pH Data_rev in Figure 5.1.

Table 5.2 Specific surface area (SSA), initial content of mineral (m_o) and kinetic parameters used for the silicate minerals in the reactive transport model. The specific surface area is obtained from (Cantucci et al., 2009) and if necessary adjusted to fit the model to the experimental data, m_0 is obtained from Table 5.2 while the kinetic parameters are found in (Palandri and Kharaka, 2004).

			Acid mechanisms			Neutral mechanism		Alkali mechanism		
	SSA	m_0	log(k25)	E_a	n	log(k25)	E_a	log(k25)	E_a	n
	m^2/g	mol	($mol/m^2/s$)	(kJ/mol)	(-)	($mol/m^2/s$)	(kJ/mol)	($mol/m^2/s$)	(kJ/mol)	(-)
Kaolinite	3.4e-6*	1.16	-11.31	65.9	0.777	-13.18	22.2	-17.05	17.9	0.472
Microcline	0.254	4.54	-10.06	51.7	0.500	-12.41	38.0	-21.20	94.1	-0.823
Quartz	0.035	190	-	-	-	-13.99	87.7	-	-	-
								Carbonate mechanism		
Ankerite [a)]	0.02	0.15	-3.19	36.1	0.500	-7.53	52.2	-5.11	34.8	0.500
Siderite[a)]	1.54e-5	7.8e-3	-3.19	36.1	0.500	-7.53	52.2	-5.11	34.8	0.500

[a)] Kinetic data for disordered dolomite

5.4 Potential geochemical reactions

5.4.1 Silica minerals

The model reproduces the fast and significant increase in the concentration of aqueous silicium upon temperature increases as well as the concentration levels at each temperature reasonable well (Figure 5.1). The silicium concentration at each temperature is controlled by a quasi-steady-state between kinetically controlled dissolution and/or precipitation of microcline, kaolinite and quartz combined with equilibrium with albite at temperatures ≥ 80°C (Figure 5.2).

Only very small amounts of silica minerals dissolves at temperatures ≤60°C (Figure 5.2). At 60°C a small conversion of microcline to kaolinite occurs:

Microcline → Kaolinite

$$KAlSi_3O_8 + H^+ + 0.5H_2O \rightarrow 0.5Al_2Si_2O_5(OH)_4 + K^+ + 2SiO_{2(aq)}$$

The conversion of Na-rich alkalifeldpar to kaolinite is previously observed at 50°C in a similar study flushing a Gassum sandstone sample from a Stenlille with synthetic Gassum formation water (Holmslykke et al., 2017a).

At 80°C the system is very close to equilibrium with both albite and microcline. Corrected bottomhole temperatures from the Farsø-1 well show a reservoir temperature of approximately 80°C. Thus it is plausible that the system is close to equilibrium with albite at this temperature. When increasing the temperature above 80°C microcline dissolves while albite

precipitates. Albitisation of microcline is known to occur in a number of sedimentary basins at deeper burial (Saigal et al., 1988). Saigal et al. (1988) conclude that the main reaction responsible for albitisation is a one-to-one replacement reaction, which can be expressed as:

$$KAlSi_3O_8 + Na^+ \rightarrow NaAlSi_3O_8 + K^+$$

When written on a molar basis, the reaction involves contemporaneous dissolution of microcline and precipitation of albite. The process involves the supply of sodium, while potassium is released to the solution. In our experiment, the supply of sodium is ensured through the injected water (Table 4.3). The release of potassium by the albitisation process is insignificant compared to the potassium content of the synthetic formation water (Table 4.3) and therefore undetectable in the chemical analysis of the effluent. As the solubility of microcline increases with increasing temperature, the albitisation process is enhanced at elevated temperatures (Figure 5.2) as also observed previously (Holmslykke et al., 2019b).

When increasing the temperature, the dissolution of quartz increases (Figure 5.2). It is well known that both the solubility of quartz and the dissolution rate increases with increasing temperature (Rimstidt and Barnes, 1980). Thus at temperatures ≥80°C significant amounts of quartz dissolves, and especially at temperatures above 100°C, the rate of quartz dissolution increases significantly as also previously observed (Holmslykke et al., 2019b; Holmslykke et al., 2017b). At 100°C as well as at 120°C dissolution of quartz is in the same order of magnitude as dissolution of microcline. Previous studies show that at while quartz dissolution and feldspar dissolution is in the same order of magnitude at 100°C, quartz dissolution dominates at 150°C (Holmslykke et al., 2019b; Holmslykke et al., 2017a).

Despite a very high saturation index for kaolinite (up to c. 4) the precipitation of kaolinite is expected to be very slow (Figure 5.2). Similar observation is made in previous studies (Holmslykke et al., 2017a). Generally, kaolinite precipitates in the early diagenesis from formation water containing significantly lower concentrations of calcium, sodium and magnesium than the used synthetic formation water and the high concentration of other cations in this study may promote formation of other clay types and have an adverse effect on the precipitation rate of kaolinite (Peng and Di, 1994).

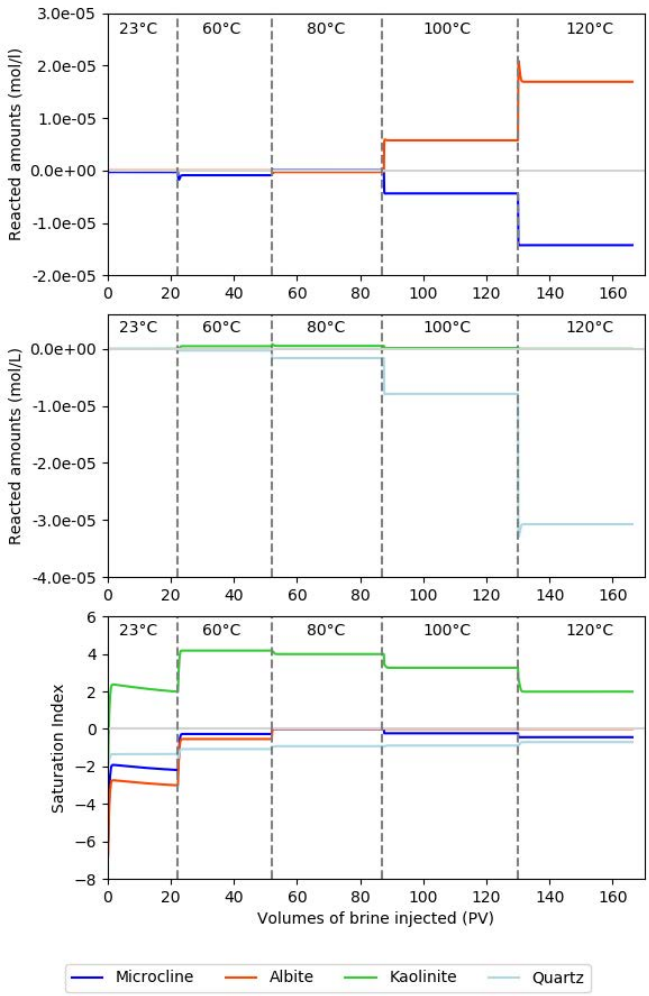

Figure 5.7 *Reacted amount and saturation index for silicates included in the PHREEQC transport model of CO_2 containing Farsø brine (Table 4.3) through a column in which kinetically controlled (Table 5.2) dissolution and/or precipitation of microcline, kaolinite, quartz, barite and ankerite is allowed and equilibrium albite at temperatures ≥80°C and with calcite at all temperatures is imposed. A positive or negative reacted amount indicate mineral precipitation or dissolution, respectively. The saturation state of the effluent is indicated by the saturation index and the possibility of dissolution and precipitation is revealed by a negative and positive value of the saturation index, respectively.*

5.4.2 Carbonates

The petrographic analysis indicates that dissolution of ankerite occurs during the experiment. This dissolution may very well be facilitated by the fact that the flooding fluid does not contain iron or manganese (Table 4.3) resulting in a synthetic formation water subsaturated with ankerite. In accordance with previous observations, ankerite with the chemical composition $CaFe_{0.3}Mg_{0.69}Mn_{0.01}(CO_3)_2$ (Deer et al., 2013) is included in the model with the kinetic parameters shown in Table 5.2. This model predicts the concentration of both aqueous iron and manganese reasonable well (Figure 5.1), particularly at temperatures below 120°C. At 120°C, the model indicates a decrease in the iron concentration after the initial increase upon raising the temperature 120°C; a decrease, which is not observed in the experimental data. The modelled decrease in the iron concentration is attributed to the fact that the amount of ankerite (m in equation (1)) has become so low that a significant fraction of the

mineral dissolves during the time of flooding with 120°C. Thus, the ratio (m/m_o) in equation (1) is reduced from 0.37 at the beginning of the flooding period with 120°C to 0.09 at the end of the flooding, leading to a reduced ankerite dissolution rate (equation (1)).

As the rate of ankerite dissolution increases and the solubility of calcite decreases with increasing temperature the solution becomes supersaturated with respect to calcite. Thus, at 60°C and higher temperatures calcite precipitates (Figure 5.3), stabilising the pH of the system:

$$CaFe_{0.3}Mg_{0.69}Mn_{0.01}(CO_3)_2 + Ca^{2+} \rightarrow 2CaCO_3 + 0.3Fe^{2+} + 0.69Mg^{2+} + 0.01Mn^{2+}$$

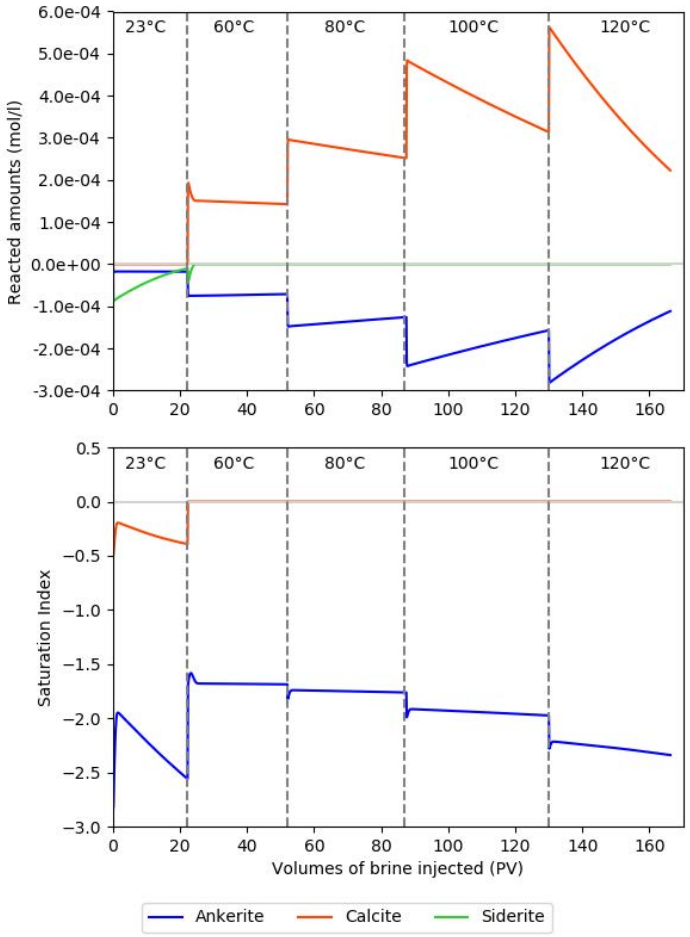

Figure 5.8 *Reacted amount and saturation index for carbonates included in the PHREEQC transport model of CO_2 containing Farsø brine (Table 4.3) through a column in which kinetically controlled (Table 5.2) dissolution and/or precipitation of microcline, kaolinite, quartz, barite and ankerite is allowed and equilibrium with albite at temperatures ≥80°C and with calcite at all temperatures is imposed. A positive or negative reacted amount indicate mineral precipitation or dissolution, respectively. The saturation state of the effluent is indicated by the saturation index and the possibility of dissolution and precipitation is revealed by a negative and positive value of the saturation index, respectively.*

The peaks in the concentration of aqueous iron at room temperature and 60°C could indicate dissolution of a reactive iron containing mineral which is present in only a small amount and hence nearly or completely dissolved during flooding with the first two temperatures of the experiment. In the model, dissolution of siderite is included with the initial amount and kinetic parameters given in Table 5.2, which gives a reasonable fit to the experimental data

(Figure 5.3). More likely, however, is the dissolution of more Fe-rich ankerite initially. Ankerite is clearly zonated (Figure 5.4) and it is possible that the outer zone may have been more iron rich than the remaining part of the mineral.

Unlike the iron concentration, the concentration of aqueous manganese peaks immediately after increasing the temperature to 80°C and 100°C (Figure 5.1). Possible explanations for these peaks in the manganese concentration could be dissolution of a more manganese rich ankerite or other manganese rich minerals and/or recrystallization of manganese oxides.

5.4.3 Barite

The model predicts the immediate increase in the concentration of aqueous barium upon a temperature increase as well as the level of barium in the effluent at the lower temperatures (up to 80°C) very well (Figure 5.1). However, at 100°C and 120°C the model underestimates the concentration of aqueous barium.

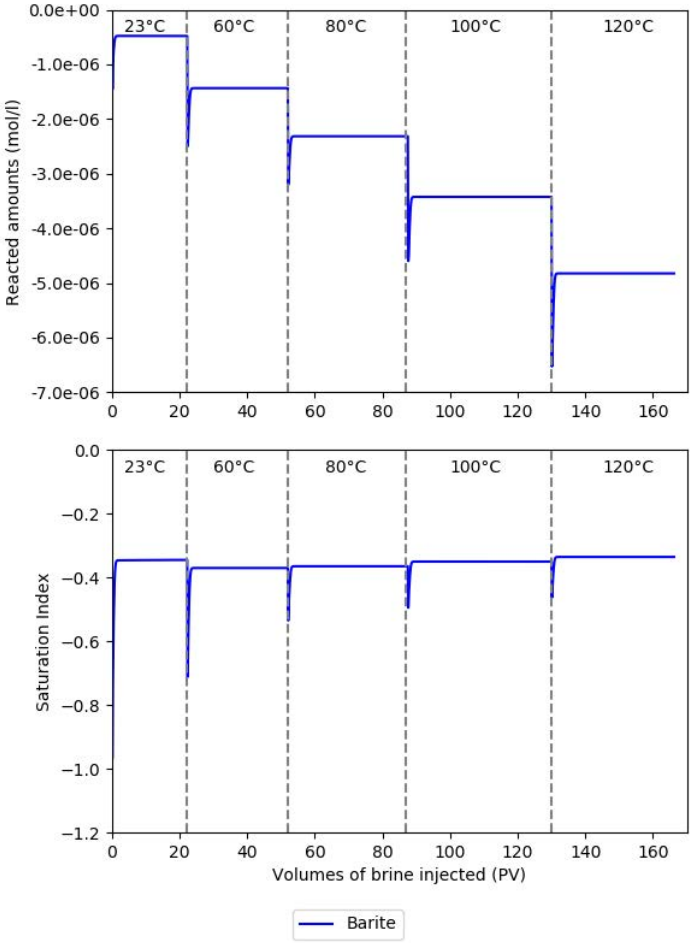

Figure 5.9 *Reacted amount and saturation index for barite included in the PHREEQC transport model of CO_2 containing Farsø brine (Table 4.3) through a column in which kinetically controlled (Table 5.2) dissolution and/or precipitation of microcline, kaolinite, quartz, barite and ankerite is allowed and equilibrium with albite at temperatures ≥80°C and with calcite at all temperatures is imposed. A positive or negative reacted amount indicate mineral precipitation or dissolution, respectively. The saturation state of the effluent is indicated by the saturation index and the possibility of dissolution and precipitation is revealed by a negative and positive value of the saturation index, respectively.*

The concentration of aqueous barium appears to be kinetically controlled by barite dissolution and the effluent remains subsaturated with respect to barite at all temperatures (Figure 5.4). Imposing equilibrium with barite in the model overestimates the barium concentration, except at 120°C. The dissolution of barite in the experiment may very well be facilitated by the absence of barium in the flooding fluid (Table 4.3). However, since the solubility of barite increases with temperature, reinjection of heated formation water may still cause barite dissolution in the reservoir.

Although trace amounts of barium is known to substitute into microcline (Bindeman and Davis, 2000), release of trace amounts of barium from the dissolving microcline can not account for the gap between the model and the experimental results at 100°C and 120°C.

It appears as if the modelled and the experimental data do not show the same temperature dependency of the barite dissolution rate. The rate expression used in this study (equation 5) is optimised for use with the Pitzer database developed by Appelo (2015). However, applying this database for the barite dissolution with identical kinetic parameters increases the barium concentration in general and do not improve the fit to the experimental data (Figure 5.1). Also, applying the rate expression given by equation 3 which is applied for the other minerals in this study does not improve the consistency between the modelled and the experimental results.

6 Implications for heat storage in the Gassum Sandstone Formation, Aalborg

The experimental data, petrographic analysis and geochemical modelling in this study indicate that reinjection of heated formation water into the Gassum formation in the Aalborg area may induce or enhance albitisation of microcline, dissolution of quartz, ankerite and barite and precipitation of calcite.

Extrapolation of the model results show that assuming a continuous injection of heated formation water into the reservoir and a constant dissolution rate in the injection period less than 0.2% of the quartz in the reservoir is likely to dissolve during a storage period of 6 months at 120°C and even less at 100°C. Thus, dissolution of quartz is not expected to deteriorate the reservoir properties noticeable. Likewise, less than 3% of the microcline present in the reservoir may potentially dissolve during storage for 6 months at 120°C and less than 1% at 100°C. This is also not expected to deteriorate the reservoir properties significantly. Similarly, the formation of albite is not expected to have major effects on the reservoir properties, since the albite precipitates inside the feldspar or as an overgrowth on the microcline and thus does not damage the reservoir. Dissolution of microcline may, however, lead to the formation of illite, especially at higher temperatures. Since illite is very fiberous the formation of illite may have a damaging effect on the permeability of the reservoir. The geochemical model indicates that the effluent is supersaturated with respect to illite and thus that illite may potentially precipitate during the experiment, although it cannot be verified by the petrographic analysis.

The main changes in the aqueous composition of the brine are increased concentrations of silicium, iron and barium caused by the dissolution processes induced by the heating. Appropriate removal of these elements e.g. by filtration in the surface facility is essential to prevent clogging of the injection well due to the risk of re-precipitation of silicium, barium and iron upon cooling of the brine to ensure a continuous heat production from the heat storage plant.

In previous studies the potential for heat storage in the deep subsurface of Denmark was investigated in the Gassum Sandstone Formation in the Stenlille area (Holmslykke et al., 2017a) and in the Bunter Sandstone Formation in the Tønder area (Holmslykke et al., 2019a) for temperatures up to 150°C. In line with the results of this study, the effects of heat storage of up to 150°C in the calcite-free Gassum Formation in the Stenlille area is expected to have only limited effects on the properties of the reservoir, and heat storage is considered possible provided operational precautions are taken. The calcite-rich Bunter Sandstone Formation was flushed with Ca-depleted synthetic formation water to avoid precipitation of calcite in the heated formation water. A significant portion of the cementing calcite dissolved during the experiment and consequently the tested Bunter Sandstone sample disintegrated after the experiment, indicating that injection of heated calcium depleted Bunter brine into the Bunter Sandstone Formation may damage the reservoir in the Tønder area. Further studies on the possibility of heat storage in Denmark should therefore focus on heat storage in calcite-rich reservoirs in which calcium-containing heated formation water is injected.

7 Conclusions

The possibility of storing heated formation water in deep hot aquifers was tested by laboratory experiment. The objective of this study was to investigate potential heat promoted dissolution and precipitation processes in the Upper Triassic – Lower Jurassic Gassum Formation in the Aalborg area. The experimental set up was designed to provide information about the geochemical reactions expected to take place upon injection of the heated formation water. Therefore the core flooding experiment was performed at formation pressure and the temperatures 23°C, 60°C, 80°C, 100°C, and 120°C. Geochemical analysis of the effluent of the flooding experiment is combined with petrographic analysis of the sandstone before and after the experiment and provide input to a geochemical numerical model that constrain and support the interpretation of the results from the laboratory experiments.

The results show that reinjection of heated formation water into the Gassum formation in the Aalborg area may induce or enhance albitisation of microcline, dissolution of quartz, ankerite and barite and precipitation of calcite. However, only small amounts of these phases are expected to dissolve and hence the dissolution processes are not expected to severely damage the reservoir properties. Since albite precipitates inside microcline grains or as overgrowths on the microcline the precipitation of albite is not expected to damage the reservoir permeability. There may, however, be a risk of illite formation, which may have a detrimental effect on the reservoir permeability due to the fibrous morphology of illite. The model results show that ilite may possibly precipitates, though precipitation of illite could not be verified by the petrographic analysis.

The main changes in the aqueous composition of the brine include increased concentrations of silicium, iron and barium caused by the dissolution processes induced partly by the heating and partly by the undersaturated (with respect to iron and barium) synthetic formation water. Appropriate removal of these elements e.g. by filtration in the surface facility is essential to prevent clogging of the injection well due to re-precipitation of silicium, barium and iron upon cooling of the brine to ensure a continuous heat production from the heat storage plant.

In conclusion, the results of this study show that the dissolution/precipitation processes that may potentially be induced by storage of heated formation water in the Gassum formation in the Aalborg area are not likely to damage the reservoir and that heat storage in this reservoir may be possible provided operational precautions are taken.

8 References

Altmaier, M., Metz, V., Neck, V., Müller, R. and Fanghänel, T. (2003) Solid-liquid equilibria of Mg(OH)2(cr) and Mg2(OH)3Cl·4H2O(cr) in the system Mg-Na-H-OH-Cl-H2O at 25°C. Geochim. Cosmochim. Acta 67, 3595-3601.

André, L., Audigane, P., Azaroual, M. and Menjoz, A. (2007) Numerical modeling of fluid–rock chemical interactions at the supercritical CO_2–liquid interface during CO_2 injection into a carbonate reservoir, the Dogger aquifer (Paris Basin, France). Energy Convers. Manage. 48, 1782-1797.

API (1998) Recommended practice for core analysis - Recommended practice 40, 2nd ed. American Petroleum Institute, Washington DC.

Appelo, C.A.J. (2015) Principles, caveats and improvements in databases for calculating hydrogeochemical reactions in saline waters from 0 to 200°C and 1 to 1000atm. Appl. Geochem. 55, 62-71.

Appelo, C.A.J. and Postma, D. (2005) Geochemistry, groundwater and pollution, 2nd ed. A. A. Balkema Publisher.

Association, A.P.H. (1975) Standard methods for the examination of water and wastewater, 14. ed ed.

Atkins, P.W. and de Paula, J. (2002) Atkins' physical chemistry, 7th ed, oxford Univ. Press.

Azaroual, M. and Fouillac, C. (1997) Experimental study and modelling of granite-distilled water interactions at 180 degrees C and 14 bars. Appl. Geochem. 12, 55-73.

Bindeman, I.N. and Davis, A.M. (2000) Trace element partitioning between plagioclase and melt: investigation of dopant influence on partition behavior. Geochim. Cosmochim. Acta 64, 2863-2878.

Blanc, P., Lassin, A. and Piantone, P. (2007) Thermoddem: A database devoted to waste minerals. . http://thermoddem.brgm.fr/, BRGM.

Brons, H.J., Griffioen, J., Appelo, C.A.J. and Zehnder, A.J.B. (1991) (Bio)geochemical reactions in aquifer material from a thermal-energy storage site. Water Res. 25, 729-736.

Cantucci, B., Montegrossi, G., Vaselli, O., Tassi, F., Quattrocchi, F. and Perkins, E.H. (2009) Geochemical modeling of CO_2 storage in deep reservoirs: The Weyburn Project (Canada) case study. Chem. Geol. 265, 181-197.

Deer, W.A., Howie, R.A. and Zussman, J. (2013) An Introduction to the Rock-Forming Minerals. Mineralogical Society of Great Britain and Ireland.

Dove, P.M. and Crerar, D.A. (1990) Kinetics of quartz dissolution in electrolyte solutions using a hydrothermal mixed flow reactor. Geochim. Cosmochim. Acta 54, 955-969.

Fanghänel, T., Neck, V. and Kim, J.I. (1996) The ion product of H2O, dissociation constants of H2CO3 and pitzer parameters in the system Na+/H+/OH−/HCO3−/CO32-/ClO4−/H2O at 25°C. J. Solution Chem. 25, 327-343.

Fu, Q., Lu, P., Konishi, H., Dilmore, R., Xu, H., Seyfried Jr, W.E. and Zhu, C. (2009) Coupled alkali-feldspar dissolution and secondary mineral precipitation in batch systems: 1. New experiments at 200 °C and 300 bars. Chem. Geol. 258, 125-135.

Gong, Q., Deng, J., Han, M., Yang, L. and Wang, W. (2012) Dissolution of sandstone powders in deionised water over the range 50–350 °C. Appl. Geochem. 27, 2463-2475.

Griffioen, J. and Appelo, C.A.J. (1993) Nature and extent of carbonate precipitation during aquifer thermal-energy storage. Appl. Geochem. 8, 161-176.

Gruber, C., Kutuzov, I. and Ganor, J. (2016) The combined effect of temperature and pH on albite dissolution rate under far-from-equilibrium conditions. Geochim. Cosmochim. Acta 186, 154-167.

Holdren, G.R. and Speyer, P.M. (1987) Reaction rate-surface area relationships during the early stages of weathering. II. Data on eight additional feldspars. Geochim. Cosmochim. Acta 51, 2311-2318.

Holmslykke, H.D., Kjoller, C. and Fabricius, I.L. (2019a) Evaluating chemical reactions upon heat storage in Danish geothermal reservoirs, European Geothermal Congress 2019, The Hague, The Netherlands

Holmslykke, H.D., Kjøller, C. and Fabricius, I.L. (2017a) Core Flooding Experiments and Reactive Transport Modeling of Seasonal Heat Storage in the Hot Deep Gassum Sandstone Formation. ACS Earth and Space Chemistry 1, 251-260.

Holmslykke, H.D., Kjøller, C. and Fabricius, I.L. (2017b) Core flooding experiments and reactive transport modeling of seasonal heat storage in the hot deep Gassum Sandstone Formation. Earth and Space Chemistry, *in press.* DOI: 10.1021/acsearthspacechem.7b00031.

Holmslykke, H.D., Kjøller, C. and Fabricius, I.L. (2019b) Evaluating chemical reactions upon heat storage in Danish geothermal reservoirs, European Geothermal Congress 2019, The Hague, The Netherlands

Hoyer, M., Hallgren, J., Eisenreich, S. and Sterling, R. (1994) Field-test results of aquifer thermal energy storage at St. Paul, Minnesota. J. Energy. Eng. 120, 67-85.

Japsen, P., Green, P.F., Nielsen, L.H., Rasmussen, E.S. and Bidstrup, T. (2007) Mesozoic-Cenozoic exhumation events in the eastern North Sea Basin: a multi-disciplinary study based on palaeothermal, palaeoburial, stratigraphic and seismic data. Basin Research 19, 451-490.

Laier, T. (1982) Fluid analysis and scaling investigations of the Gassum Formation water of Farsø 1. Geological Survey of Denmark and Greenland.

Laier, T. (2008) Chemistry of Danish saline formation waters relevant for core fluid experiments – Fluid chemistry data for lab experiments related to CO_2 storage on deep aquifers. GEUS report 2008/48, Geological Survey of Denmark and Greenland, Copenhagen.

Moore, D.E., Morrow, C.A. and Byerlee, J.D. (1983) Chemical reactions accompanying fluid flow through granite held in a temperature gradient. Geochim. Cosmochim. Acta 47, 445-453.

Nielsen, L.H. (2003) Late Triassic-Jurassic development of the Danish Basin and the Fennoscandian Border Zone, southern Scandinavia, in: Ineson, J.R., Surlyk, F. (Eds.), The Jurassic of Denmark and Greenland, Geological Survey of Denmark and Greenland Bulletin 1, pp. 459-526.

Nielsen, L.H. and Japsen, P. (1991) Deep wells in Denmark 1935-1990. Lithostratigraphic subdivision, Geological Survey of Denmark A 31, p. 179 pp.

Palandri, J.L. and Kharaha, Y.K. (2004) A compilation of rate parameters of water-mineral interaction kinetics for application to geochemical modeling, U.S. Geological Survey Water-Resources Investigations Report 04-1068.

Palandri, J.L. and Kharaka, Y.K. (2004) A Compilation of Rate Parameters of Water-mineral Interaction Kinetics for Application to Geochemical Modeling. National Energy Technology Laboratory, U.S. Department of the Interior, U.S. Geological Survey.

Parkhurst, D.L. and Appelo, C.A.J. (2013) Description of input and examples for PHREEQC version 3 - A computer program for speciation, batch-reaction, one-dimensional transport, and inverse geochemical calculations, U.S. Geological Survey Techniques and Methods.

Peng, F.F. and Di, P. (1994) Effect of Multivalent Salts—Calcium and Aluminum on the Flocculation of Kaolin Suspension with Anionic Polyacrylamide. J. Colloid Interface Sci. 164, 229-237.

Perlinger, J.A., Almendinger, J.E., Urban, N.R. and Eisenreich, S.J. (1987) Groundwater geochemistry of aquifer thermal energy storage - Long term test cycle. Water Resour. Res. 23, 2215-2226.

Pitzer, K.S. (1981) Characteristics of very concentrated aqueous solutions. Phys. Chem. Earth 13, 249-272.

Plummer, L.N., Parkhurst, D.L., Fleming, G.W. and Dunkle, S.A. (1988) A computer program incorporating Pitzer's equations for calculation of geochemical reactions in brines, Water-Resources Investigations Report, - ed.

Rimstidt, J.D. and Barnes, H.L. (1980) The kinetics of silica-water reactions. Geochim. Cosmochim. Acta 44, 1683-1699.

Saigal, G.C., Morad, S., Bjorlykke, K., Egeberg, P.K. and Aagaard, P. (1988) Diagenetic albitization of detrital K-feldspar in Jurassic, Lower Cretaceous, and Tertiary clastic reservoir rocks from offshore Norway; I, Textures and origin. J. Sediment. Res. 58, 1003-1013.

Schembre, J.M. and Kovscek, A.R. (2005) Mechanism of formation damage at elevated temperature. J. Energy Resour. technol. Trans. ASME 127, 171-180.

Schepers, A. and Milsch, H. (2013) Dissolution-precipitation reactions in hydrothermal experiments with quartz-feldspar aggregates. Contrib. Mineral. Petrol. 165, 83-101.

Tenthorey, E., Scholz, C.H., Aharonov, E. and Leger, A. (1998) Precipitation sealing and diagenesis - 1. Experimental results. J. Geophys. Res.: Solid Earth 103, 23951-23967.

Weibel, R., Olivarius, M., Friis, H., Kristensen, L., Hjuler, M.L., Kjoller, C., Pedersen, P.K., Boyce, A., Mathiesen, A. and Nielsen, L.H. (2017a) Climatic influence on early and burial diagenesis in Triassic and Jurassic sandstones from the Norwegian – Danish Basin. The Depositional record 3, 60-91.

Weibel, R., Olivarius, M., Kristensen, L., Friis, H., Hjuler, M.L., Kjøller, C., Mathiesen, A. and Nielsen, L.H. (2017b) Predicting permeability of low-enthalpy geothermal reservoirs: A case study from the Upper Triassic – Lower Jurassic Gassum Formation, Norwegian–Danish Basin. Geothermics 65, 135-157.

Zhen-Wu, B.Y., Dideriksen, K., Olsson, J., Raahauge, P.J., Stipp, S.L.S. and Oelkers, E.H. (2016) Experimental determination of barite dissolution and precipitation rates as a function of temperature and aqueous fluid composition. Geochim. Cosmochim. Acta 194, 193-210.